Interference of FZD2 suppresses proliferation, vasculogenic mimicry and stemness in glioma cells via blocking the Notch/NF-κB signaling pathway

YUGE RAN[1*], SHUAI HAN[2*], DONGXUE GAO[3], XIAOBO CHEN[1] and CHAN LIU[1]

[1]Department of Radiotherapy, Affiliated Hospital of Hebei University, Baoding, Hebei 071000, P.R. China;
[2]Department of Medicine, Batai Biopharmaceutical Co., Ltd., Beijing 102600, P.R. China;
[3]Proton Therapy Center, Cancer Hospital Chinese Academy of Medical Sciences, Langfang, Hebei 065000, P.R. China

Received August 29, 2023; Accepted March 22, 2024

DOI: 10.3892/etm.2024.12662

Abstract. Frizzled family protein 2 (FZD2) is widely associated with tumor development and metastasis. The present study aimed to gain an insight into the role and regulatory mechanism of FZD2 in glioma. The expression level of FZD2 in normal astrocyte and glioma cells was determined by reverse transcription-quantitative PCR and western blotting, and cell transfection was conducted for FZD2 expression knockdown. Malignant behaviors including cell proliferation, migration and invasion, vasculogenic mimicry (VM) and cell stemness were determined using Cell Counting Kit-8, 5-Ethynyl-2'-deoxyuridine (EdU) staining, colony formation, wound healing, Transwell, 3D culturing and sphere formation assays. The expression levels of proteins related to stemness, epithelial-mesenchymal transition (EMT) and Notch/NF-κB signaling were measured by western blotting. Then, the Notch agonist, Jagged-1 (JAG), was adopted for rescue experiments. The results demonstrated that FZD2 was highly expressed in glioma cells. Interference of FZD2 expression suppressed the proliferation of glioma cells, as evidenced by the reduced cell viability and the number of EdU^+ cells and colonies. Meanwhile, the reduced sphere formation ability and decreased protein expression of Nanog, Sox2 and Oct4 following FZD2 knockdown confirmed that FZD2 repressed cell stemness in glioma. Additionally, FZD2 knockdown suppressed the migration, invasion, EMT and VM formation capabilities of glioma cells, and also blocked the Notch/NF-κB signaling pathway. Furthermore, activation of Notch by JAG treatment partially reversed the aforementioned FZD2 knockdown-mediated changes in glioma cell malignant behaviors. In conclusion, FZD2 may contribute to glioma progression through activating the Notch/NF-κB signaling pathway, providing a plausible therapeutic target for the treatment of glioma.

Correspondence to: Dr Chan Liu, Department of Radiotherapy, Affiliated Hospital of Hebei University, 212 Yuhua Road, Baoding, Hebei 071000, P.R. China
E-mail: liuchan841014@163.com

*Contributed equally

Key words: glioma, frizzled family protein 2, vasculogenic mimicry, stemness, Notch

Introduction

Glioma is the most prevalent type of primary tumor in the brain, accounting for 81% of central nervous system malignancies, and is one of the leading causes of mortality worldwide (1). Glioma is a highly heterogeneous group of tumors, including astrocytomas [World Health Organization (WHO) grade I-IV], ependymomas (WHO grade II-III) and oligodendrogliomas (2). Despite major efforts to optimize early diagnosis and treatment, conventional therapies including surgical resection, radiotherapy and chemotherapy, possess limited improvements in the prognosis of patients with glioma, and the median overall survival time of patients with grade IV glioma is ~15 months, along with a poor 5-year survival rate of <10% (3). Hence, it is of great importance and urgency to explore the molecular mechanisms underlying the progression of glioma.

Vasculogenic mimicry (VM), initially described in uveal melanomas by Maniotis *et al* (4) in 1999, is considered a novel form of blood supply independent of blood vessels, attributed to its formation of microvascular channels composed of tumor cells, distinguishing it from the traditional angiogenetic process involving vascular endothelium (5). VM occurs in numerous malignancies, including prostate cancer, breast cancer, ovarian cancer and glioma (6-9). It has been reported that VM formation promotes tumor cell proliferation and invasion, and typically predicts a poor prognosis in patients with glioma (10,11). Therefore, VM is regarded as a novel target for glioma therapy.

The frizzled family proteins (FZDs, including FZD1-10) are 10-transmembrane receptors for Wnt ligands, and are not only involved in embryogenesis and development but also in cancer progression (12). Of note, FZD2 is a highly conserved signaling molecule that also belongs to the G protein-coupled receptor family. Accumulating evidence has revealed the

aberrant expression of FZD2 in various malignancies, including tongue squamous cell carcinoma, breast cancer and hepatocellular carcinoma, in which FZD2 acts as an oncogene (13-15). By contrast, FZD2 serves as a tumor-suppressor gene in salivary adenoid cystic carcinoma (16), demonstrating that FZD2 has a dual role in different types of tumors. A recent report based on RNA-sequencing data from clinical glioma samples revealed that FZD1/2/5/7/8 was significantly highly expressed in tumor tissues. Furthermore, the FZD2 expression level increased as the progression of the glioma increased from grade II to grade IV, and FZD2 was suggested to be a novel independent predictor of unfavorable prognosis in glioma (17). Notably, FZD2 has been discovered to promote the VM phenotype in hepatocellular carcinoma, indicating a potential association between FZD2 and VM formation (13). Nevertheless, the specific role of FZD2 in glioma progression has not been completely understood.

Therefore the present study aimed to explore the molecular function of FZD2 in glioma progression, its regulatory effect on VM formation during glioma progression and its potential regulatory mechanism. The present study may therefore provide novel ideas for developing therapeutic strategies for glioma treatment.

Materials and methods

Cell culture and treatment. Human astrocyte HEB cells (4th passage) were obtained from Jennio Biotech Co., Ltd. The human glioma cell lines, A172 (cat. no. iCell-h002), T98G (cat. no. iCell-h210) and LN229 (cat. no. iCell-h124), and the U87MG glioblastoma cell line of unknown origin (cat. no. iCell-h224) were obtained from iCell Bioscience Inc. and authenticated by STR analysis. All cells were cultured in Dulbecco's Modified Eagle Medium (Thermo Fisher Scientific, Inc.) supplemented with 10% fetal bovine serum (FBS; Thermo Fisher Scientific, Inc.) and 1% penicillin/streptomycin mixture (Invitrogen; Thermo Fisher Scientific, Inc.) in a humidified incubator with 5% CO_2 at 37˚C.

In addition, to explore the relevant mechanisms of action, the Notch agonist Jagged-1 (JAG) peptide (50 μg/ml; R&D Systems, Inc.) was used to treat U87MG glioblastoma cells at 37˚C for 48 h.

Reverse transcription-quantitative PCR (RT-qPCR). Total RNA was extracted from cells utilizing TRIzol reagent (Invitrogen; Thermo Fisher Scientific, Inc.) in-line with the manufacturer's guidelines, followed by RT to cDNA using SuperScript Reverse Transcriptase (Invitrogen; Thermo Fisher Scientific, Inc.) according to the manufacturer's protocols. Subsequently, qPCR was conducted using FastStart Universal Probe Master (Roche Diagnostics) and a Bio-Rad CFX96 Real-Time PCR System (Bio-Rad Laboratories, Inc.). The thermocycling conditions were as follows: Preheating at 90˚C for 10 min, followed by 30 cycles of 95˚C for 30 sec, 55˚C for 30 sec and 72˚C for 60 sec, with a final elongation step at 72˚C for 10 min and 4˚C on hold. The primer sequences used in the present study were as follows: FZD2 forward, 5'-AGTTCTATCCGCTGGTGAAGGT-3' and reverse, 5'-GCCCAGAAACTTGTAGCTGAGA-3'; Nanog forward, 5'-GTGATTTGTGGGCCTGAAGA-3' and reverse, 5'-ACACAGCTGGGTGGAAGAGA-3'; Sox2 forward, 5'-ACACCAATCCCATCCACACT-3' and reverse, 5'-GCAAACTTCCTGCAAAGCTC-3'; Oct4 forward, 5'-AGCCCTCATTTCACCAGGCC-3' and reverse, 5'-CCCCCACAGAACTCATACGG-3'; GAPDH forward, 5'-CAGGAGGCATTGCTGATGAT-3' and reverse, 5'-GAAGGCTGGGGCTCATTT-3'. Target gene expression was calculated using the $2^{-\Delta\Delta Cq}$ method (18), normalized to GAPDH.

Western blotting. Total proteins were extracted from cells utilizing RIPA buffer (Beyotime Institute of Biotechnology), followed by quantification using a BCA Protein Assay Kit (Beyotime Institute of Biotechnology) to determine the protein concentration. The proteins (30 μg/lane) were fractionated by electrophoresis using a 10% SDS-polyacrylamide gel, transferred to polyvinylidene difluoride membranes (MilliporeSigma), blocked with 5% non-fat milk at room temperature for 1 h and probed using primary antibodies against FZD2 (cat. no. 24272-1-AP; 1:500; Proteintech Group, Inc.), Nanog (cat. no. ab109250; 1:1,000; Abcam), Sox2 (cat. no. ab92494; 1:1,000; Abcam), Oct4 (cat. no. ab200834; 1:10,000; Abcam), E-cadherin (cat. no. ab40772; 1:1,000; Abcam), N-cadherin (cat. no. ab76011; 1:5,000; Abcam), Vimentin (cat. no. ab92547; 1:1,000; Abcam), Snail (cat. no. ab216347; 1:1,000; Abcam), N1ICD (cat. no. ab52301; 1:1,000; Abcam), Hes1 (cat. no. ab71559; 1:1,000; Abcam), phosphorylated (p-)NF-κB p65 (cat. no. ab239882; 1:1,000; Abcam), NF-κB p65 (cat. no. ab207297; 1:1,000; Abcam) and GAPDH (cat. no. ab9485; 1:2,500; Abcam) at 4˚C overnight. On the following day, membranes were incubated with a horseradish peroxidase-conjugated secondary antibody (cat. no. ab6721; 1:3,000; Abcam) at room temperature for 2 h. Immunoreactivity was developed using Western Chemiluminescent HRP substrate (MilliporeSigma) and semi-quantified using ImageJ software 1.52 (National Institutes of Health).

Cell transfection. Short hairpin (sh)RNAs targeting FZD2, including sh-FZD2-1 (5'-CATCCTATCTCAGCTACAA-3') and sh-FZD2-2 (5'-CCGACTTCACGGTCTACAT-3'), were synthesized by Shanghai GenePharma Co., Ltd., and the empty shRNA plasmid (pGPU6/Neo) served as the negative control (sh-NC; Shanghai GenePharma, Co., Ltd.). The shRNAs (500 ng/μl) were transfected into U87MG glioblastoma cells using Lipofectamine 3000 reagent (Invitrogen; Thermo Fisher Scientific, Inc.) in-line with the manufacturer's guidelines. The cells in the control group were those that did not receive transfection. After 48 h, the transfection efficiency was determined by RT-qPCR and western blotting.

Cell Counting Kit-8 (CCK-8) assay. A CCK-8 kit (Dojindo Laboratories, Inc.) was utilized to determine the cell proliferation ability. In brief, U87MG glioblastoma cells were inoculated into 96-well plates and incubated at 37˚C under 5% CO_2 for 24, 48 and 72 h. Then, 10 μl CCK-8 solution was added to each well and the cells were incubated for another 2 h. Finally, the absorbance of each well at 450 nm was detected using a microplate reader (BioTek; Agilent Technologies, Inc.).

5-Ethynyl-2'-deoxyuridine (EdU) staining assay. U87MG cells were cultured in 96-well plates and treated with 100 μl EdU (50 μM; Abcam). After incubation at 37˚C under 5% CO_2 for 2 h, the cells were fixed in 4% paraformaldehyde for 15 min at room temperature and permeabilized with 0.5% Triton X-100 for 15 min at room temperature. Subsequently, cells were incubated with 100 μl EdU reaction cocktail (cat. no. ab219801; Abcam) for 20 min at room temperature, and 4,6-diamino-2-phenylindole (DAPI) was used to counterstain the nuclei for 15 min at room temperature. Finally, images were captured using a fluorescence microscope (Olympus Corporation).

Colony formation assay. U87MG cells ($1x10^3$) were inoculated into 6-well plates and cultured at 37˚C under 5% CO_2 for 10 days. During this period, the culture medium was refreshed every 2-3 days. Finally, the colonies consisting of >50 cells were fixed with 4% paraformaldehyde for 20 min at room temperature and then stained with 0.1% crystal violet for 20 min at room temperature for visualization and counting using ImageJ software 1.52 (National Institutes of Health).

Wound healing assay. U87MG cells were seeded into 6-well plates and incubated at 37˚C under 5% CO_2. Once 100% confluency was reached, a straight scratch was generated using a 200-μl pipette tip. The cells were then washed with PBS and incubated in serum-free medium at 37˚C under 5% CO_2 for 48 h. Images at 0 and 48 h were captured using a bright-field microscope (Olympus Corporation). The migration rate was determined according to the width of the wounds measured using ImageJ software 1.52 (National Institutes of Health).

Transwell assay. The cell invasion potential was assessed using Matrigel-coated (37˚C for 30 min) Transwell assay inserts with a 8-μm pore size (Corning, Inc.). $1x10^5$ U87MG cells were resuspended in serum-free medium and inoculated into the upper chamber of a Transwell plate. Then, 500 μl complete medium containing 10% FBS was added to the lower chamber. After incubation for 48 h at 37˚C, the invaded cells were fixed with 4% paraformaldehyde for 20 min at room temperature then stained with 0.1% crystal violet for 10 min at room temperature. The invaded cells were observed under a bright-field microscope (Olympus Corporation).

Sphere formation assay. U87MG cells ($1x10^3$) were resuspended in cancer stemness medium (cat. no. 12400-024; Gibco; Thermo Fisher Scientific, Inc.) containing B27, 20 ng/ml basic fibroblast growth factor and 20 ng/ml epidermal growth factor, then seeded into 24-well ultra-low attachment plates (Corning, Inc.) and incubated at 37˚C under 5% CO_2. Following a 10-day incubation, cell spheres with a diameter >75 μm were observed using a bright-field microscope (Olympus Corporation).

3D culturing. The *in vitro* VM formation potential of U87MG cells was evaluated by 3D culturing as previously described (11). In brief, 96-well plates were pre-coated with Matrigel (BD Biosciences) at 37˚C for 30 min. U87MG cells ($1x10^5$) were resuspended in serum-free medium and seeded on the Matrigel. After incubation at 37˚C under 5% CO_2 for 8 h, images were captured using a bright-field microscope (Olympus Corporation), and tube formation was assessed manually.

Immunofluorescence assay. U87MG cells were fixed in 4% paraformaldehyde for 15 min at room temperature and permeabilized with 0.5% Triton X-100 for 15 min at room temperature. Then, after blocking with 10% normal goat serum (Beijing Solarbio Science & Technology Co., Ltd.) at 37˚C for 30 min, the cells were probed with anti-VE-cadherin antibody (cat. no. ab313632; 1:50; Abcam) at 4˚C overnight. On the following day, the cells were incubated with Goat Anti-Rabbit IgG (Alexa Fluor® 488) preadsorbed antibody (cat. no. ab150081; 1:1,000; Abcam) at 37˚C for 1 h in the dark. DAPI was used to counterstain the nuclei for 15 min at room temperature. Finally, images were captured using a fluorescence microscope (Olympus Corporation).

Bioinformatic and statistical analysis. Quantitative data are presented as the mean ± standard deviation. All statistical analyses were conducted using GraphPad Prism 8 (Dotmatics). Comparisons were conducted using one-way ANOVA followed by Tukey's post hoc test. To assess the role of FZD2 in glioma/glioblastoma, the expression of FZD2 in glioblastoma was explored using the Gene Expression Profiling Interactive Analysis (GEPIA; http://gepia.cancer-pku.cn/) (19) and UALCAN (https://ualcan.path.uab.edu/index.html) databases (20). The unpaired Student's t-test was applied for difference comparisons. In addition, the Chinese Glioma Genome Atlas (CGGA; http://www.cgga.org.cn/) (21) was applied to assess the survival probability in patients with grade I-III glioma (cut-off value of 50% to determine high and low FZD2 status) $P<0.05$ was considered to indicate a statistically significant difference.

Results

FZD2 is upregulated in glioma tissues and cells. To uncover the role of FZD2 in glioma/glioblastoma, the expression of FZD2 in glioma was first explored using the GAPIA and UALCAN databases. According to these databases, the FZD2 expression level in the tumor tissues of patients with glioma was higher than that in the normal tissues (Fig. 1A and B). In addition, based on data from the CGGA, it was found that high expression of FZD2 was positively associated with poor survival probability in patients with grade I-III glioma (Fig. 1C). To confirm the aberrant high level of FZD2 in glioma, the expression of FZD2 was also detected in multiple glioma/glioblastoma cell lines and astrocyte HEB cells. As shown in Fig. 1D and E, both the mRNA and protein expression levels of FZD2 were significantly higher in glioma/glioblastoma cell lines (A172, U87MG, T98G and LN229) compared with HEB cells, and the highest levels were observed in U87MG glioblastoma cells.

Interference of FZD2 restricts the proliferation and stemness of U87MG cells. To clarify the regulatory role of FZD2 in glioma, shRNA cell transfections were conducted using U87MG cells. Compared with the sh-NC group, the expression level of FZD2 in the sh-FZD2-1 and sh-FZD2-2 groups was significantly reduced (Fig. 2A and B). sh-FZD2-1 was adopted in the subsequent experiments due to the more

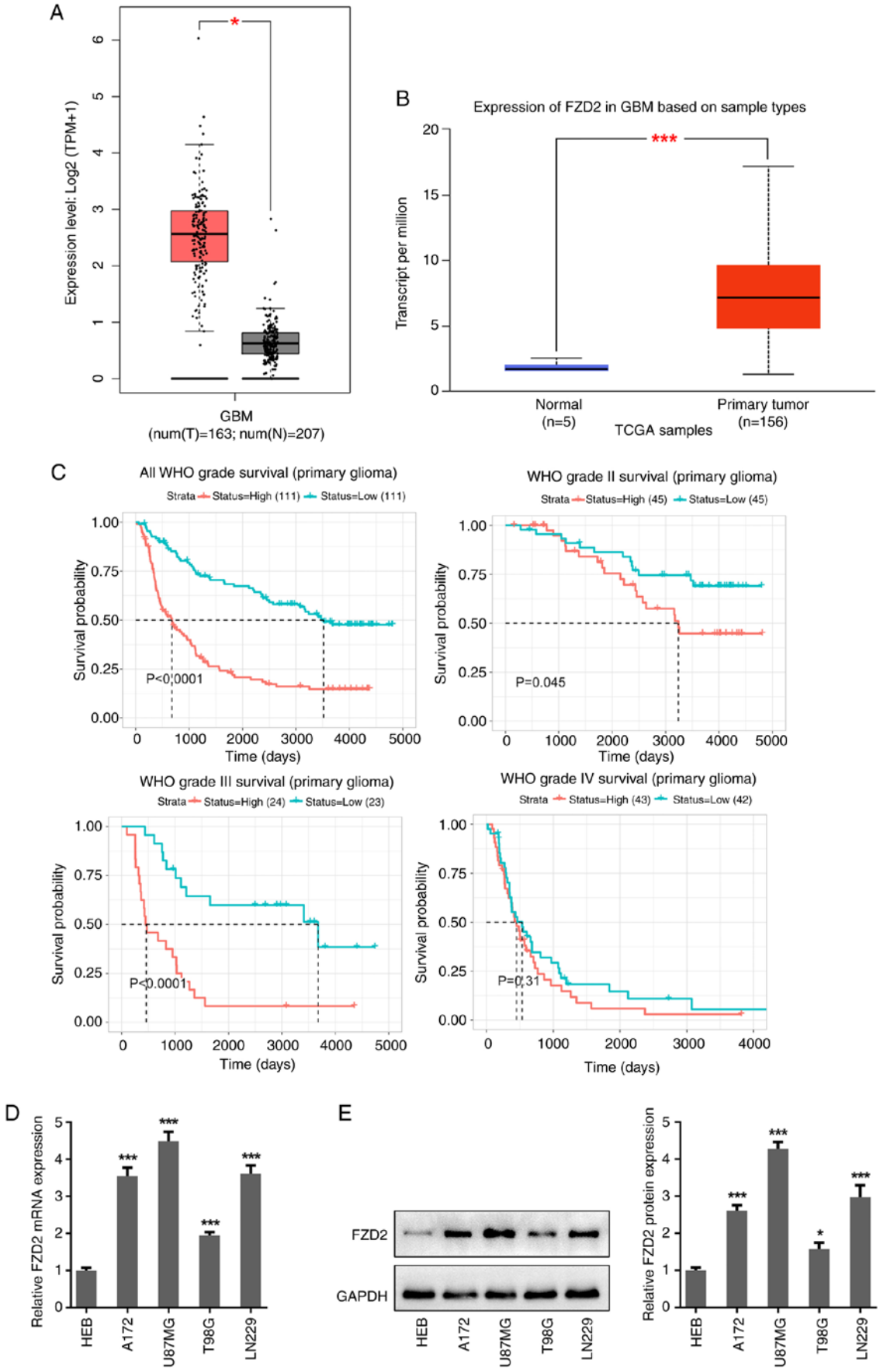

Figure 1. FZD2 is upregulated in glioma tissues and cells. Analysis of FZD2 expression in glioma using the (A) GEPIA and (B) UALCAN databases. (C) The Chinese Glioma Genome Atlas database was used to predicted the impact of FZD2 expression on the survival probability of patients with different grades of glioma. (D) mRNA and (E) protein expression levels of FZD2 were detected using reverse transcription-quantitative PCR and western blotting, respectively. *P<0.05, ***P<0.001 vs. HEB. FZD2, frizzled family protein 2; WHO, World Health Organization; GBM, glioblastoma; TPM, transcripts per million; TCGA, The Cancer Genome Atlas; T, tumor; N, normal.

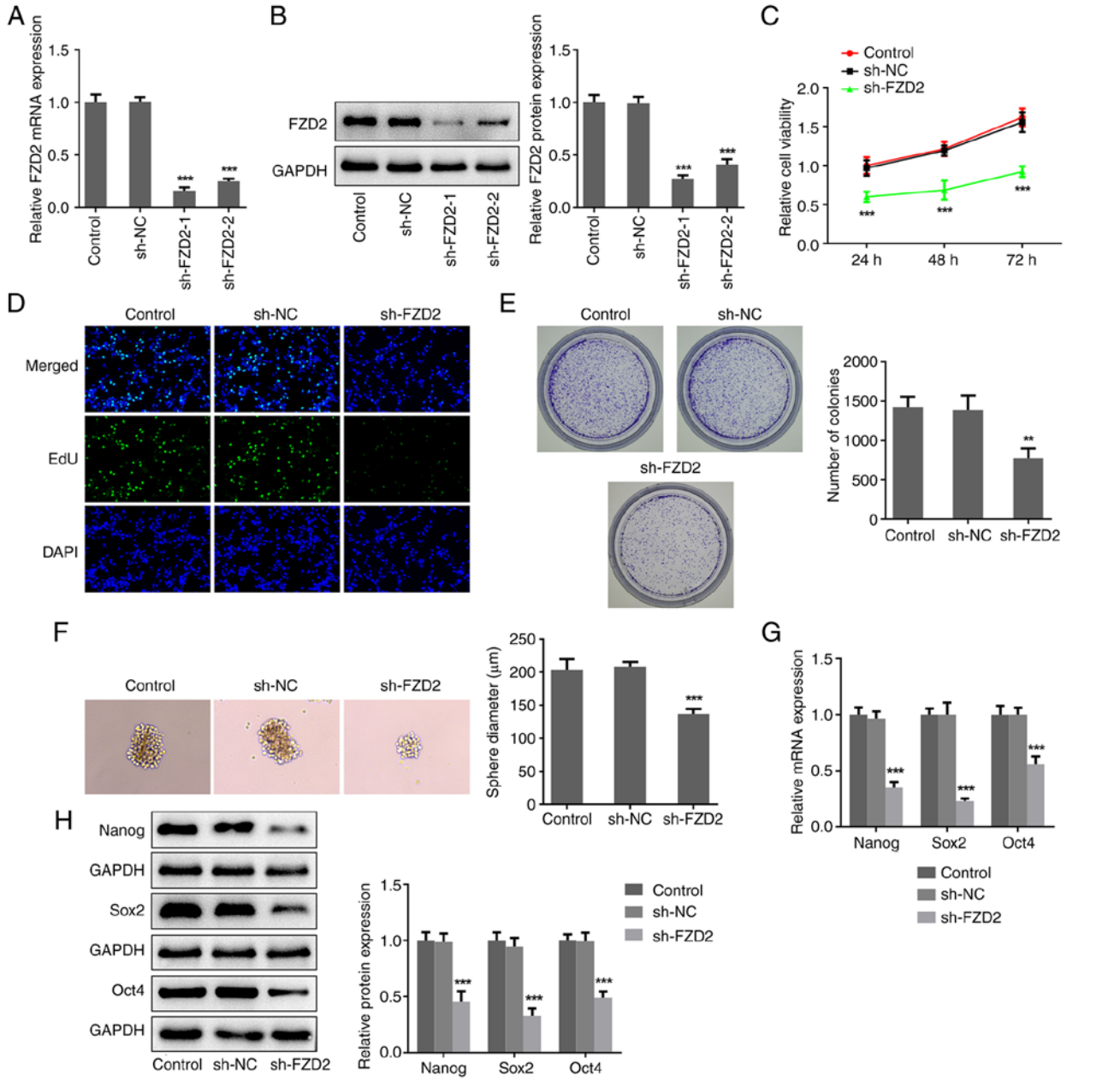

Figure 2. Interference of FZD2 restricts the proliferation and stemness of U87MG cells. U87MG cells were transfected with sh-NC and sh-FZD2-1/2, and the (A) mRNA and (B) protein expression levels of FZD2 were detected by RT-qPCR and western blotting, respectively. (C) Cell Counting Kit-8, (D) EdU staining (magnification, x200) and (E) colony formation assays were performed to assess cell proliferation. (F) Sphere formation assay was conducted to assess cell stemness (magnification, x100). (G) mRNA and (H) protein expression levels of Nanog, Sox2 and Oct4 were detected by RT-qPCR and western blot, respectively. **P<0.01, ***P<0.001 vs. control. EdU, 5-Ethynyl-2'-deoxyuridine; sh, short hairpin; NC, negative control; FZD2, frizzled family protein 2; DAPI, 4,6-diamino-2-phenylindole.

optimized transfection efficacy. Thereafter, a series of *in vitro* experiments were conducted to assess the impacts of FZD2 on cellular biological activities. According to the results from the CCK-8, EdU staining and colony formation assays (Fig. 2C-E), the relative cell viability, the number of EdU$^+$ cells and the number of colonies in the sh-FZD2 group were significantly decreased compared with the sh-NC group, indicating that interference with FZD2 expression greatly restricted the proliferation ability of U87MG cells. In addition, it was observed that significantly smaller spheres were formed by FZD2-knockdown U87MG cells compared with the control cells (Fig. 2F), meaning that FZD2 knockdown lowered the sphere formation ability, thereby alleviating cell stemness in glioma. Furthermore, it was also discovered that FZD2 knockdown significantly lowered both the mRNA and protein expression levels of Nanog, Sox2 and Oct4 (Fig. 2G and H), the critical factors of cell stemness. Taken together, these results demonstrated that FZD2 knockdown may lower glioma cell proliferation ability and stemness.

Interference of FZD2 represses the migration, invasion and VM formation capabilities of U87MG cells. In addition, the impacts of FZD2 on cell migration, invasion and VM formation in glioma was also investigated. As shown in Fig. 3A-C,

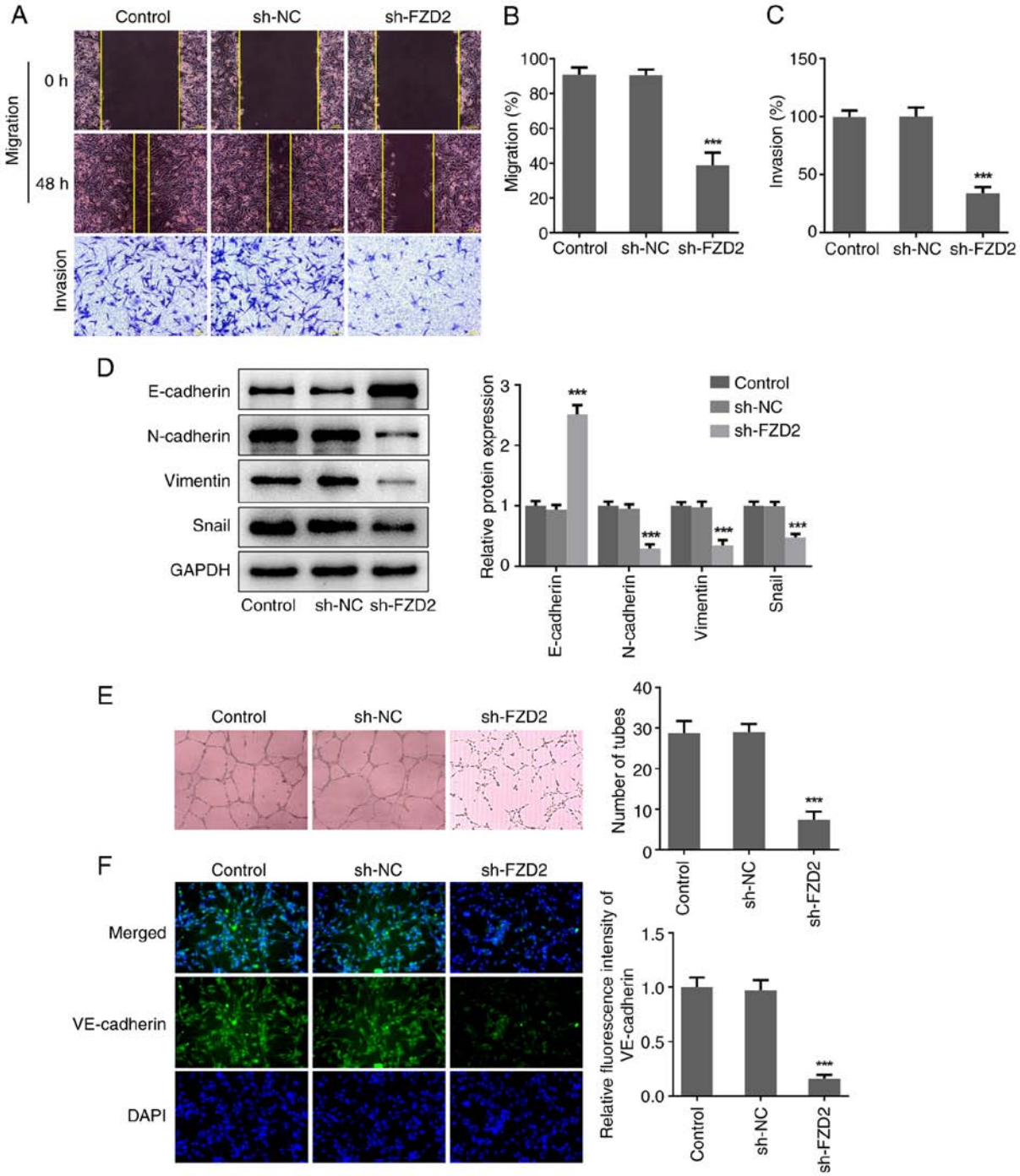

Figure 3. Interference of FZD2 represses the migration, invasion and VM formation capabilities of U87MG cells. (A) U87MG cells were transfected with sh-NC and sh-FZD2, wound-healing and Transwell assays were conducted to assess cell migration and invasion, respectively (magnification, x100). (B) The migration rate and (C) invasion rate were quantified. (D) Protein expression levels of E-cadherin, N-cadherin, Vimentin and Snail were examined by western blotting. (E) *In vitro* 3D culturing model was constructed to assess VM formation ability (magnification, x100). (F) Cell immunofluorescence assay was performed to detect VE-cadherin expression (magnification, x200). ***P<0.001. VM, vasculogenic mimicry; sh, short hairpin; NC, negative control; FZD2, frizzled family protein 2; DAPI, 4,6-diamino-2-phenylindole.

compared with the sh-NC group, the wound closure and cell invasion rates of the sh-FZD2 group were significantly lower, suggesting that FZD2 knockdown inhibited the migration and invasion abilities of U87MG cells. Meanwhile, FZD2 knockdown significantly increased the protein expression level of E-cadherin but reduced the protein expression levels of N-cadherin, Vimentin and Snail (Fig. 3D), reflecting an inhibitory effect of FZD2 knockdown on epithelial-mesenchymal transition (EMT) in glioma cells. In addition, U87MG cells formed typical channels and tube-like structures in the *in vitro* 3D culturing model, while the number of formed tubes were significantly reduced when FZD2 expression was knocked down (Fig. 3E). Meanwhile, the significantly reduced VE-cadherin level following FZD2 knockdown further confirmed that interference of FZD2 expression restricted the VM formation ability of glioma cells (Fig. 3F).

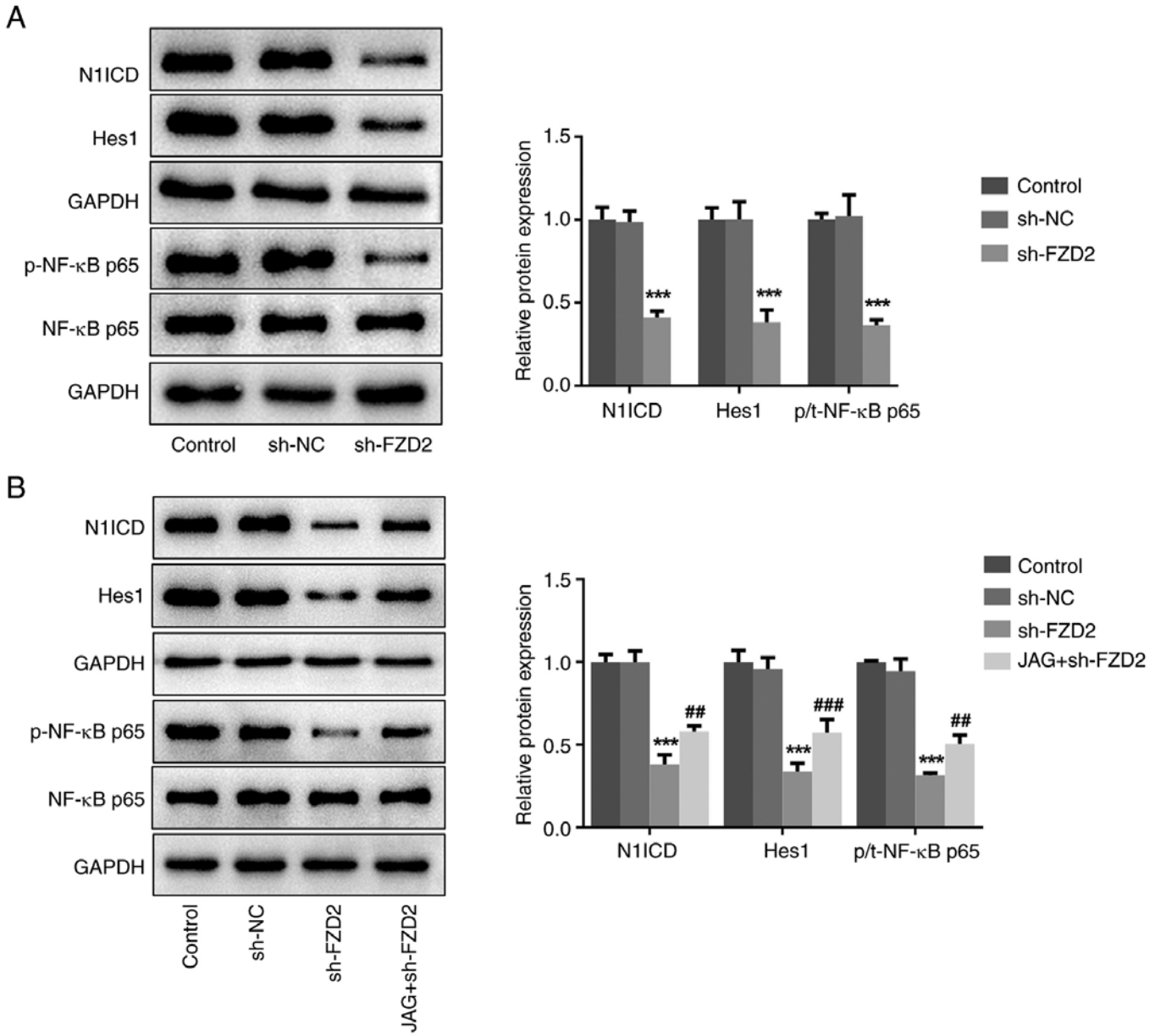

Figure 4. Interference of FZD2 blocks the Notch/NF-κB signaling pathway in U87MG cells. (A) U87MG cells were transfected with sh-NC or sh-FZD2 and the expression levels of Notch/NF-κB signaling-associated proteins were measured using western blotting. (B) U87MG cells were transfected with sh-FZD2 with or without treatment with the Notch agonist, JAG, and the expression levels of Notch/NF-κB signaling-associated proteins were measured using western blotting. ***P<0.001 vs sh-NC; $^{##}$P<0.01, $^{###}$P<0.001 vs sh-FZD2. sh, short hairpin; NC, negative control; FZD2, frizzled family protein 2; JAG, Jagged-1; p-, phosphorylated; t-, total; N1ICD, Notch 1 intracellular domain.

Interference of FZD2 blocks the Notch/NF-κB signaling pathway in U87MG cells. Next, an attempt was made to elucidate the underlying molecular basis behind the regulatory role of FZD2 in glioma. Since FZD2 can induce Notch signaling and Notch signaling has a critical role in regulating the malignant metastasis of glioma (22,23), the impact of FZD2 on Notch signaling in glioma was also explored. As shown in Fig. 4A, FZD2 knockdown significantly inhibited the protein expression levels of intracellular domain of NOTCH1 receptor (N1ICD), Hes1 and p-NF-κB p65, revealing that FZD2 knockdown restricted the activation of Notch/NF-κB signaling in glioma cells. To confirm the importance of Notch signaling underlying FZD2-mediated glioma progression, the Notch agonist JAG peptide was used to treat sh-FZD2-transfected U87MG cells. The western blotting results revealed that the inhibitory effect of FZD2 knockdown on the N1ICD, Hes1 and p-NF-κB p65 protein expression levels was partially weakened by JAG treatment (Fig. 4B), further proving the FZD2 regulation of the Notch/NF-κB signaling pathway in glioma.

Activation of Notch abolishes the FZD2 knockdown-mediated antioncogenic effects in U87MG cells. Finally, to highlight the importance of the Notch/NF-κB signaling pathway underlying FZD2-mediated glioma, cellular biological behaviors were again examined but in the presence of JAG. As shown in Fig. 5A-C, activation of Notch by JAG significantly weakened the antiproliferation property of FZD2 knockdown in glioma, as evidenced by the elevated

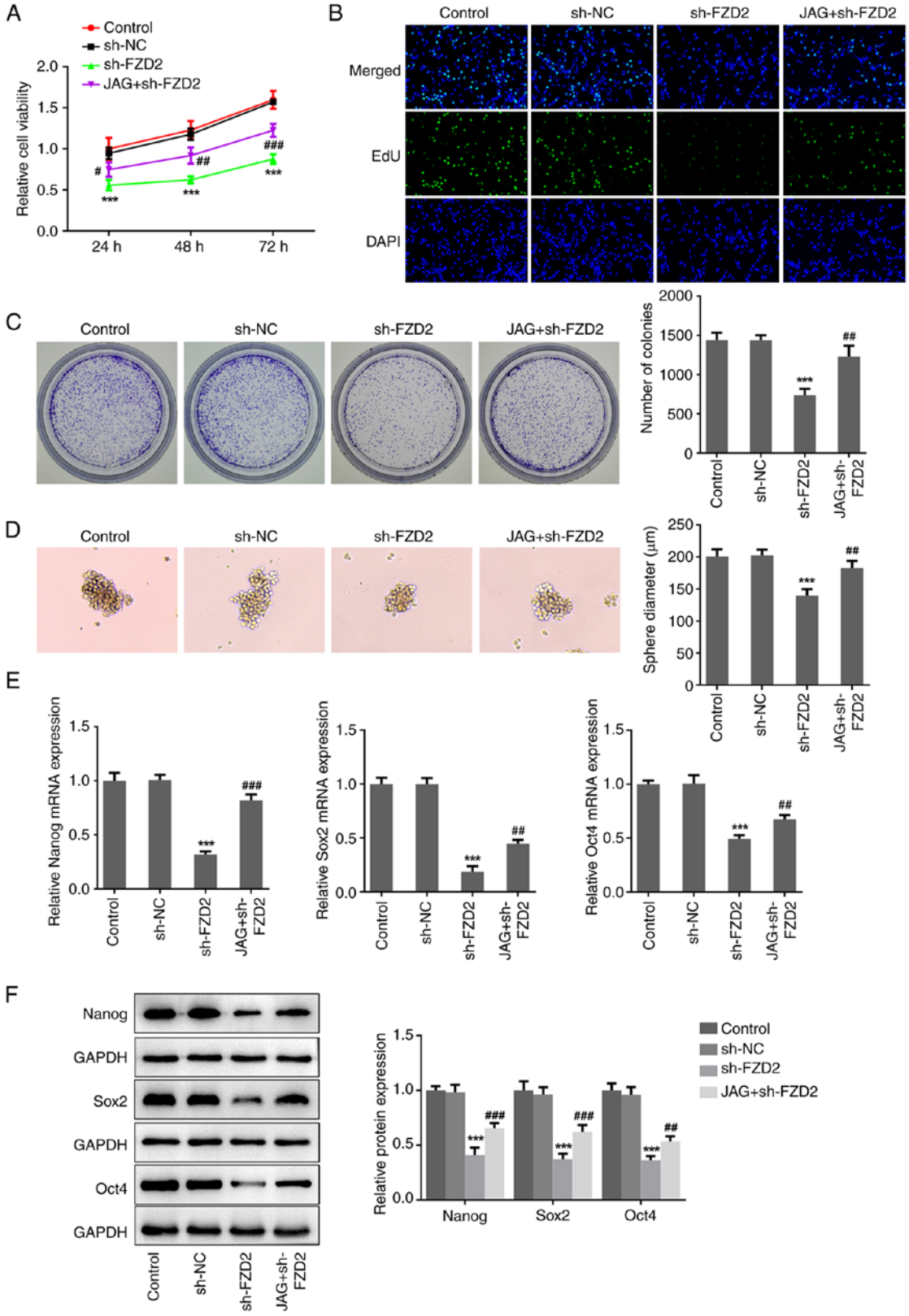

Figure 5. Activation of Notch abolishes the inhibitory effects of FZD2 knockdown on cell proliferation and stemness in U87MG cells. U87MG cells were transfected with sh-FZD2 with or without treatment of the Notch agonist, JAG. (A) Cell Counting Kit-8, (B) EdU staining (magnification, x200) and (C) colony formation assays were performed to assess cell proliferation ability. (D) Sphere formation assay was conducted to assess cell stemness (magnification, x100). (E) mRNA and (F) protein expression levels of Nanog, Sox2 and Oct4 were detected by reverse transcription- quantitative PCR and western blotting, respectively. ***P<0.001 vs sh-NC; $^{\#}$P<0.05, $^{\#\#}$P<0.01, $^{\#\#\#}$P<0.001 vs sh-FZD2. sh, short hairpin; NC, negative control; FZD2, frizzled family protein 2; JAG, Jagged-1.

cell viability, the number of EdU^{+} cells and the number of colonies in the JAG+sh-FZD2 group compared with the sh-FZD2 group. Meanwhile, JAG treatment partially abolished the suppressive effects of FZD2 knockdown on sphere

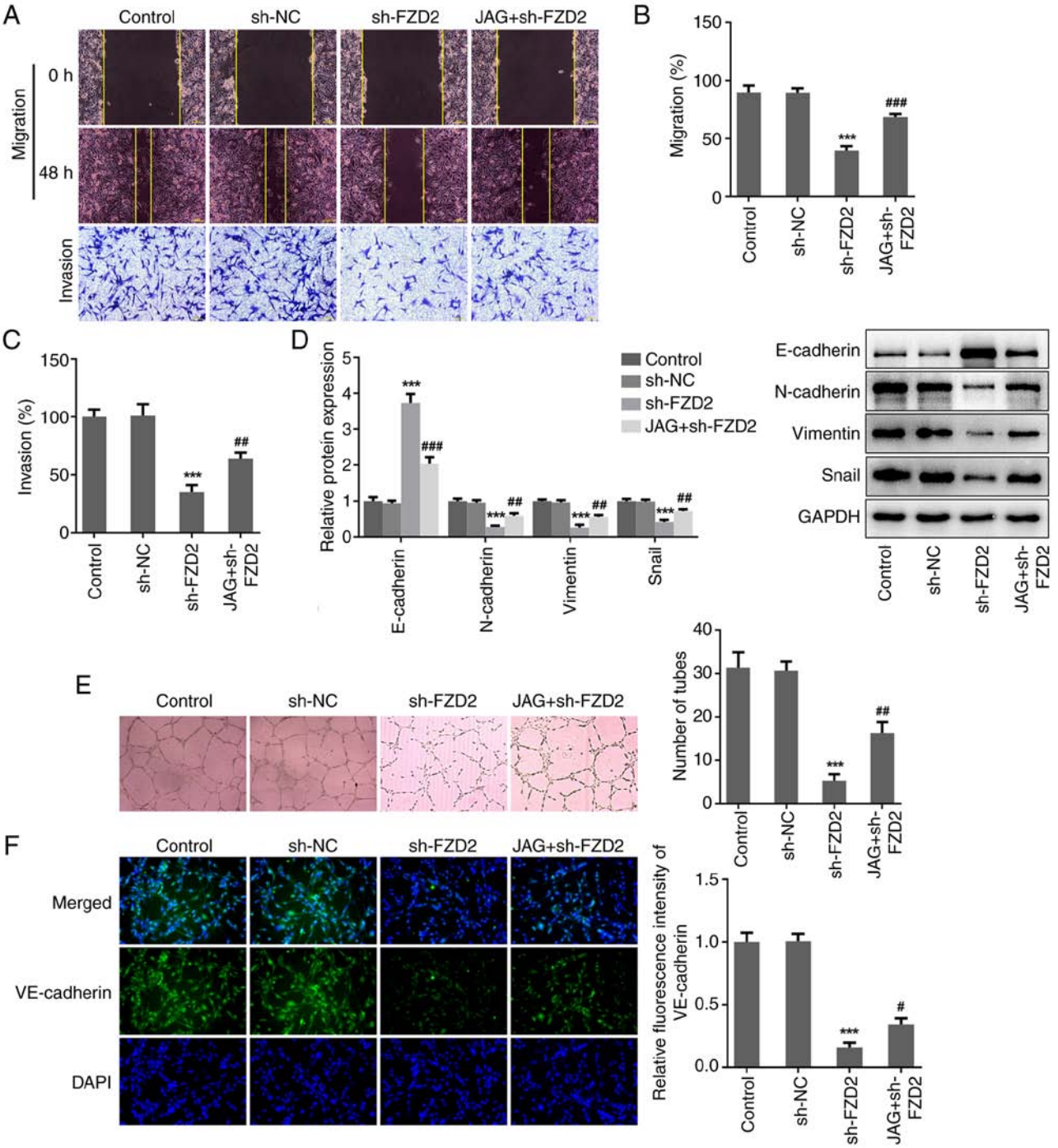

Figure 6. Activation of Notch abolishes the inhibitory effects of FZD2 knockdown on cell migration, invasion and VM formation in U87MG cells. (A) U87MG cells were transfected with sh-FZD2 with or without treatment with the Notch agonist, JAG. Wound healing and Transwell assays were conducted to assess cell migration and invasion, respectively (magnification, x100). (B) The migration rate and (C) invasion rate were quantified. (D) Protein expression levels of E-cadherin, N-cadherin, Vimentin and Snail were examined by western blotting. (E) *In vitro* 3D culturing model was constructed to assess VM formation ability (magnification, x100). (F) Cell immunofluorescence assay was performed to detect VE-cadherin expression. (magnification, x200). ***P<0.001 vs sh-NC; $^{\#}$P<0.05, $^{\#\#}$P<0.01, $^{\#\#\#}$P<0.001 vs sh-FZD2. VM, vasculogenic mimicry; sh, short hairpin; NC, negative control; FZD2, frizzled family protein 2; JAG, Jagged-1; DAPI, 4,6-diamino-2-phenylindole.

formation ability and the expression of Nanog, Sox2 and Oct4 (Fig. 5D-F), indicating that the FZD2 knockdown-associated lowered cell stemness in glioma was hindered by the activation of Notch. Additionally, JAG treatment also significantly facilitated wound closure, elevated the rate of cell invasion and upregulated N-cadherin, Vimentin and Snail protein expression and downregulated E-cadherin protein expression in sh-FZD2-transfeted U87MG cells (Fig. 6A-D), reflecting that JAG partially hindered the regulatory function of FZD2 knockdown on cell migration, invasion and EMT in glioma cells. Furthermore, compared with the sh-FZD2 group, the elevated number of tubes and VE-cadherin expression level in the JAG + sh-FZD2 group confirmed that JAG also abolished the inhibitory effect of FZD2 knockdown on VM formation in glioma cells (Fig. 6E and F).

Discussion

In the present study, FZD2 was shown to be highly expressed in glioma cells. Functionally, interference of FZD2 expression led to inhibition of the malignant biological properties of glioma cells including proliferation, migration, invasion, EMT, VM formation and stemness. More notably, the importance of the Notch/NF-κB signaling pathway in the oncogenic role of FZD2 in glioma was confirmed.

Vascularization is crucial for the growth and metastasis of tumors. Antiangiogenic therapy is a new treatment method for glioma; however, the current antiangiogenic drugs, including irinotecan and bevacizumab, are far from satisfactory due to the existence of VM (24,25). Hence, investigating the drugs/targets that restrict VM formation may be a new avenue in the treatment of glioma, which has attracted attention in recent years. For instance, Zhu *et al* (26) attributed the activity of celastrol, a potential antitumor drug against glioma, to the inhibition of VM formation and angiogenesis in glioma. Pan *et al* (27) indicated a potential role for migration-inducing gene-7 (Mig-7) as a target in the treatment of glioma as silencing Mig-7 inhibited cell invasion and VM formation in glioma cells. In terms of FZD2, a study reported by Ou *et al* (13) revealed that FZD2 could promote the clinically relevant VM phenotype while FZD2 knockdown suppressed the VM phenotype in hepatocellular carcinoma, which was partially responsible for the oncogenic action of FZD2 in hepatocellular carcinoma cells, preliminarily demonstrating the impact of FZD2 on VM. Accordingly, in the present study, the results also revealed that FZD2 knockdown significantly repressed the VM formation of glioma cells. Meanwhile, FZD2 knockdown also significantly restricted the malignant activities of glioma cells by inhibiting the proliferation, migration and invasion capabilities of glioma cells. Therefore, the oncogenic role of FZD2 in glioma may be associated with VM. Additionally, a small number of cancer cells possessing stem cell-like properties are the strongest angiogenic cells in tumors, accounting for the development and recurrence of tumors (28). In particular, it has been observed that glioma stem-like cells may act as progenitors for VM formation, highlighting the association between VM and stemness in glioma (29). Furthermore, a previous study reported that FZD2-mediated malignant behaviors in hepatocellular carcinoma were associated with VM and stemness (13). In addition, FZD2 knockdown disturbed migration, invasion and the mesenchymal-like phenotype of breast cancer cells, confirming the oncogenic role of FZD2 in breast cancer via the promotion of cell mesenchymal-like stemness (15). In agreement with these existing findings, the present study also demonstrated the inhibitory effects of FZD2 knockdown on the stemness phenotype of glioma cells. Taken together, the oncogenic role of FZD2 in glioma may be associated with VM and stemness phenotypes, and the inhibitory effects of FZD2 knockdown on the malignant behaviors of glioma cells, including proliferation, migration, invasion and EMT, may be partially associated with the restriction of these VM and stemness phenotypes.

Notch signaling is a highly conserved pathway which has a critical role in maintaining embryonic development and adult tissue homeostasis and is involved in regulating multiple cellular processes, including cell proliferation and differentiation, stem cell maintenance and cell fate decisions (30,31). Disrupted Notch signaling has been implicated in various pathological diseases, including cancer. It has been proposed that Notch is activated in the classical and proneural subtypes of glioma, and that Notch signaling cross-talk with NF-κB p65 contributes to glioma growth (32,33). The Notch signaling pathway can promote migration, invasion, growth and the self-renewal of glioma cells, and inhibition of Notch is suggested to be a promising target for restricting tumor growth during glioma development (32-34). For instance, NFIX circular RNA can promote glioma progression through upregulating Notch signaling (35). Notably, it has also been demonstrated that Notch signaling can exert a dual role in glioma, serving as an oncogene or a tumor suppressor depending on the intratumoral (stem) cell heterogeneity, disease stage and crosstalk with other signaling pathways (36). In the present study, it was found that FZD2 knockdown, which exerted antioncogenic activity in glioma cells, significantly inhibited activation of the Notch signaling pathway. Furthermore, JAG treatment partially inhibited the antioncogenic activity of FZD2 knockdown in glioma cells, confirming that inactivation of Notch signaling may be beneficial to inhibit glioma development, and that Notch might be partially responsible for the regulatory functions of FZD2 in the malignant behaviors of glioma.

However, there were some limitations in the present study. First, this study was only conducted using *in vitro* cellular experiments to demonstrate the regulatory role of FZD2 in glioma, and clinical validation and *in vivo* verification will be beneficial to prove the significance of FZD2 in glioma. Secondly, this study only demonstrated that the regulatory role of FZD2 was dependent on the Notch/NF-κB signaling pathway, while there might be multiple factors and pathways responsible for this oncogenic role in glioma. Thus, more potential regulatory mechanisms should be explored in further research. Finally, how FZD2 affected the Notch/NF-κB pathway remains unclear. According to the String (https://cn.string-db.org/) and GENEMANIA (http://genemania.org/) websites, multiple proteins were found to interact with FZD2, and of note, FZD2 was closely related to Wnt pathway-related factors, such as Wnt5a. The Wnt pathway is one of the important pathways affecting Notch signaling output and the regulatory role of Wnt-Notch signaling in cancer progression has been widely reported (37-39). The Wnt pathway might act as a mediator between FZD2 and the Notch/NF-κB pathway, but this hypothesis requires future exploration.

In conclusion, taken together, the findings of the present study may deepen the understanding of FZD2 in glioma. An oncogenic role of FZD2 in glioma was identified and FZD2 knockdown suppressed the proliferation, migration, invasion, VM formation and stemness of glioma cells. In addition, FZD2 may contribute to the malignant biological behaviors of glioma cells through activating the Notch/NF-κB signaling pathway. The present study therefore may provide novel ideas for developing therapeutic strategies for the treatment of glioma.

Acknowledgements

Not applicable.

Funding

No funding was received.

Availability of data and materials

The data generated in the present study may be requested from the corresponding author.

Authors' contributions

CL designed the experiments; YR, SH, DG and XC collected and analyzed the data; YR and SH interpreted the data and drafted the manuscript. CL revised the manuscript. CL and YR confirm the authenticity of all the raw data. All authors read and approved the final version of the manuscript.

Ethics approval and consent to participate

Not applicable.

Patient consent for publication

Not applicable.

Competing interests

The authors declare that they have no competing interests.

References

1. Xu S, Tang L, Li X, Fan F and Liu Z: Immunotherapy for glioma: Current management and future application: Cancer Lett 476: 1-12, 2020.
2. Louis DN, Perry A, Reifenberger G, von Deimling A, Figarella-Branger D, Cavenee WK, Ohgaki H, Wiestler OD, Kleihues P and Ellison DW: The 2016 world health organization classification of tumors of the central nervous system: A summary. Acta Neuropathol 131: 803-820, 2016.
3. Omuro A and DeAngelis LM: Glioblastoma and other malignant gliomas: A clinical review. JAMA 310: 1842-1850, 2013.
4. Maniotis AJ, Folberg R, Hess A, Seftor EA, Gardner LM, Pe'er J, Trent JM, Meltzer PS and Hendrix MJ: Vascular channel formation by human melanoma cells in vivo and in vitro: Vasculogenic mimicry. Am J Pathol 155: 739-752, 1999.
5. Wei X, Chen Y, Jiang X, Peng M, Liu Y, Mo Y, Ren D, Hua Y, Yu B, Zhou Y, *et al*: Mechanisms of vasculogenic mimicry in hypoxic tumor microenvironments. Mol Cancer 20: 7, 2021.
6. Lim D, Do Y, Kwon BS, Chang W, Lee MS, Kim J and Cho JG: Angiogenesis and vasculogenic mimicry as therapeutic targets in ovarian cancer. BMB Rep 53: 291-298, 2020.
7. Li H, Wang D, Yi B, Cai H, Wang Y, Lou X, Xi Z and Li Z: SUMOylation of IGF2BP2 promotes vasculogenic mimicry of glioma via regulating OIP5-AS1/miR-495-3p axis. Int J Biol Sci 17: 2912-2930, 2021.
8. Morales-Guadarrama G, García-Becerra R, Méndez-Pérez EA, García-Quiroz J, Avila E and Díaz L: Vasculogenic mimicry in breast cancer: Clinical relevance and drivers. Cells 10: 1758, 2021.
9. Luo Y, Yang Z, Yu Y and Zhang P: HIF1α lactylation enhances KIAA1199 transcription to promote angiogenesis and vasculogenic mimicry in prostate cancer. Int J Biol Macromol 222: 2225-2243, 2022.
10. Liu Y, Li F, Yang YT, Xu XD, Chen JS, Chen TL, Chen HJ, Zhu YB, Lin JY, Li Y, *et al*: IGFBP2 promotes vasculogenic mimicry formation via regulating CD144 and MMP2 expression in glioma. Oncogene 38: 1815-1831, 2019.
11. Cai HP, Wang J, Xi SY, Ni XR, Chen YS, Yu YJ, Cen ZW, Yu ZH, Chen FR, Guo CC, *et al*: Tenascin-cmediated vasculogenic mimicry formation via regulation of MMP2/MMP9 in glioma. Cell Death Dis 10: 879, 2019.
12. Li Y, Liu Z and Zhang Y: Expression and prognostic impact of FZDs in pancreatic adenocarcinoma. BMC Gastroenterol 21: 79, 2021.
13. Ou H, Chen Z, Xiang L, Fang Y, Xu Y, Liu Q, Hu Z, Li X, Huang Y and Yang D: Frizzled 2-induced epithelial-mesenchymal transition correlates with vasculogenic mimicry, stemness, and Hippo signaling in hepatocellular carcinoma. Cancer Sci 110: 1169-1182, 2019.
14. Huang L, Luo EL, Xie J, Gan RH, Ding LC, Su BH, Zhao Y, Lin LS, Zheng DL and Lu YG: FZD2 regulates cell proliferation and invasion in tongue squamous cell carcinoma. Int J Biol Sci 15: 2330-2339, 2019.
15. Yin P, Wang W, Gao J, Bai Y, Wang Z, Na L, Sun Y and Zhao C: Fzd2 Contributes to breast cancer cell mesenchymal-like stemness and drug resistance. Oncol Res 28: 273-284, 2020.
16. Ding LC, Huang XY, Zheng FF, Xie J, She L, Feng Y, Su BH, Zheng DL and Lu YG: FZD2 inhibits the cell growth and migration of salivary adenoid cystic carcinomas. Oncol Rep 35: 1006-1012, 2016.
17. Huang K, Xu H, Han L, Xu R, Xu Z and Xie Y: Identification of therapeutic targets and prognostic biomarkers among frizzled family genes in glioma. Front Mol Biosci 9: 1054614, 2023.
18. Livak KJ and Schmittgen TD: Analysis of relative gene expression data using real-time quantitative PCR and the 2(-Delta Delta C(T)) method. Methods 25: 402-408, 2001.
19. Li C, Tang Z, Zhang W, Ye Z and Liu F: GEPIA2021: Integrating multiple deconvolution-based analysis into GEPIA. Nucleic Acids Res 49: W242-W246, 2021.
20. Chandrashekar DS, Karthikeyan SK, Korla PK, Patel H, Shovon AR, Athar M, Netto GJ, Qin ZS, Kumar S, Manne U, *et al*: UALCAN: An update to the integrated cancer data analysis platform. Neoplasia 25: 18-27, 2022.
21. Zhao Z, Zhang KN, Wang Q, Li G, Zeng F, Zhang Y, Wu F, Chai R, Wang Z, Zhang C, *et al*: Chinese glioma genome atlas (CGGA): A comprehensive resource with functional genomic data from Chinese glioma patients. Genomics Proteomics Bioinformatics 19: 1-12, 2021.
22. Tuluhong D, Chen T, Wang J, Zeng H, Li H, Dunzhu W, Li Q and Wang S: FZD2 promotes TGF-β-induced epithelial-to-mesenchymal transition in breast cancer via activating notch signaling pathway. Cancer Cell Int 21: 199, 2021.
23. Li Q, Wang J, Ma X, Wang M and Zhou L: POFUT1 acts as a tumor promoter in glioblastoma by enhancing the activation of notch signaling. J Bioenerg Biomembr 53: 621-632, 2021.
24. Yu S, Ruan X, Liu X, Zhang F, Wang D, Liu Y, Yang C, Shao L, Liu Q, Zhu L, *et al*: HNRNPD interacts with ZHX2 regulating the vasculogenic mimicry formation of glioma cells via linc00707/miR-651-3p/SP2 axis. Cell Death Dis 12: 153, 2021.
25. Vredenburgh JJ, Desjardins A, Herndon JE II, Dowell JM, Reardon DA, Quinn JA, Rich JN, Sathornsumetee S, Gururangan S, Wagner M, *et al*: Phase II trial of bevacizumab and irinotecan in recurrent malignant glioma. Clin Cancer Res 13: 1253-1259, 2007.
26. Zhu Y, Liu X, Zhao P, Zhao H, Gao W and Wang L: Celastrol suppresses glioma vasculogenic mimicry formation and angiogenesis by blocking the PI3K/Akt/mTOR signaling pathway. Front Pharmacol 11: 25, 2020.
27. Pan Z, Zhu Q, You W, Shen C, Hu W and Chen X: Silencing of Mig-7 expression inhibits in-vitro invasiveness and vasculogenic mimicry of human glioma U87 cells. Neuroreport 30: 1135-1142, 2019.
28. Singh SK, Hawkins C, Clarke ID, Squire JA, Bayani J, Hide T, Henkelman RM, Cusimano MD and Dirks PB: Identification of human brain tumour initiating cells. Nature 432: 396-401, 2004.
29. Medina MA, Muñoz-Chápuli R and Quesada AR: Challenges of antiangiogenic cancer therapy: Trials and errors, and renewed hope. J Cell Mol Med 11: 374-382, 2007.
30. Hori K, Sen A and Artavanis-Tsakonas S: Notch signaling at a glance. J Cell Sci 126: 2135-2140, 2013.
31. Siebel C and Lendahl U: Notch signaling in development, tissue homeostasis, and disease. Physiol Rev 97: 1235-1294, 2017.
32. Hai L, Zhang C, Li T, Zhou X, Liu B, Li S, Zhu M, Lin Y, Yu S, Zhang K, *et al*: Notch1 is a prognostic factor that is distinctly activated in the classical and proneural subtype of glioblastoma and that promotes glioma cell survival via the NF-κB(p65) pathway. Cell Death Dis 9: 158, 2018.
33. Zhang X, Chen T, Zhang J, Mao Q, Li S, Xiong W, Qiu Y, Xie Q and Ge J: Notch1 promotes glioma cell migration and invasion by stimulating β-catenin and NF-κB signaling via AKT activation. Cancer Sci 103: 181-190, 2012.

34. Yi L, Zhou X, Li T, Liu P, Hai L, Tong L, Ma H, Tao Z, Xie Y, Zhang C, *et al*: Notch1 signaling pathway promotes invasion, self-renewal and growth of glioma initiating cells via modulating chemokine system CXCL12/CXCR4. J Exp Clin Cancer Res 38: 339, 2019.
35. Xu H, Zhang Y, Qi L, Ding L, Jiang H and Yu H: NFIX circular RNA promotes glioma progression by regulating miR-34a-5p via notch signaling pathway. Front Mol Neurosci 11: 225, 2018.
36. Parmigiani E, Taylor V and Giachino C: Oncogenic and tumor-suppressive functions of NOTCH signaling in glioma. Cells 9: 2304, 2020.
37. Gao J, Fan L, Zhao L and Su Y: The interaction of notch and Wnt signaling pathways in vertebrate regeneration. Cell Regen 10: 11, 2021.
38. Krishnamurthy N and Kurzrock R: Targeting the Wnt/beta-catenin pathway in cancer: Update on effectors and inhibitors. Cancer Treat Rev 62: 50-60, 2018.
39. Borggrefe T, Lauth M, Zwijsen A, Huylebroeck D, Oswald F and Giaimo BD: The Notch intracellular domain integrates signals from Wnt, hedgehog, TGFβ/BMP and hypoxia pathways. Biochim Biophys Acta 1863: 303-313, 2016.